

An Automatic Graph-based Method for Retinal Blood Vessel Classification

Behdad Dashtbozorg^{1,2}
Behdad.dashtbozorg@fe.up.pt

Ana Maria Mendonça^{1,2}
amendon@fe.up.pt

Aurélio Campilho^{1,2}
campilho@fe.up.pt

¹ INEB - Instituto de Engenharia Biomédica,
Rua do Campo Alegre, 823, 4150-180 Porto, Portugal

² Faculdade de Engenharia, Universidade do Porto,
Rua Dr. Roberto Frias, 4200-465 Porto, Portugal.

Abstract

In this paper, we present an automatic approach to classify retinal vessels into artery and vein classes by analyzing the extracted graph from the vasculature tree and deciding on the type of intersection points (bifurcation, crossing or meeting points). The results obtained by the proposed method were compared with manual classification on 40 images of the INSPIRE-AVR dataset.

1 Introduction

Retinal vessels can be affected by many diseases. In conditions such as diabetic retinopathy, the blood vessels often show abnormalities at early stages [1]. Retinal vessel dilatation is a well-known phenomenon in diabetes and significant dilatation and elongation of arterioles, venules, and their macular branches occur in the development of diabetic macular edema that can be linked to hydrostatic pressure changes [2]. Changes in retinal blood vessels are also associated with hypertension and other cardio-vascular conditions [3]. A sign that has been shown to be related to cardiovascular diseases is the generalized arteriolar narrowing, usually expressed by the Arteriolar-to-Venular diameter Ratio (AVR). Small changes in the AVR are associated with increases in the risk for stroke, cerebral atrophy, cognitive decline, myocardial infarct [4] and also it can be affected by other diseases, like diabetic retinopathy and retinopathy of prematurity [5].

In order to develop an automatic system for measuring the AVR, besides detecting the optic disc (OD) and segmenting the retinal vasculature, one of the main challenges is to classify the vessels as artery or vein (A/V classification) [6]. Several works on vessel classification have been proposed in the literature [7]-[10]. However the automated classification of the retinal vessels into arteries and veins has received limited attention and it is still an open task in the retinal image processing field. Within this context, in this paper we propose an automatic method to classify the retinal vessels as artery or vein (A/V classification).

2 Methodology

There are some visual and geometrical features that enables the discrimination between veins and arteries. The arteries are bright red and veins are darker. In general, artery calibers are smaller than veins calibers. The arteries have thicker walls, which reflect the light as a shiny central reflex strip [11]. There are methods that explore these properties for classification purposes [8]-[10]. Another characteristic of the retinal vessel tree is that at least in the region near the optic disc, veins rarely cross veins and arteries rarely cross arteries, but both types can bifurcate to narrower vessels and also veins and arteries can cross each other [7], [11]. In our method, we assume where each intersection point is either a point where a vessel bifurcates to narrower parts or a point that a vein and an artery crosses each other.

Figure 1 depicts the block diagram of our approach for A/V classification. After vessel segmentation and centerline extraction, the main phases are: 1) graph generation; 2) graph analysis; and 3) vessel classification. The algorithm first classifies the veins and arteries by analyzing the vessel tree as a graph which has been obtained by making a decision on the type of each intersection point (graph nodes); then, vessel segments (graph links) are classified into two different classes, and finally the A/V classes are assigned to the graph links by extracting a set of features and using a linear classifier. In the following we detail each phase of the method.

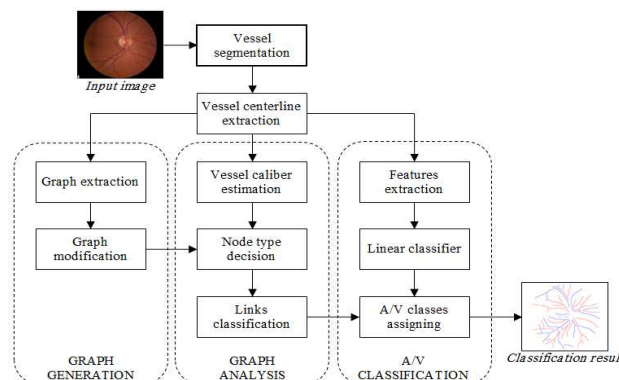


Figure 1: Block diagram of the method for A/V classification.

2.1 Graph generation

A graph is a simple representation of the vascular tree, where each node denotes an intersection point in the vascular tree and each link corresponds to a vessel segment between two intersection points.

We used the segmentation method proposed by Mendonça *et al.* [12] which has good performance also in the detection and segmentation of thin vessels. An illustrative result for vessel segmentation is shown in Figure 2(b). Afterward we used the segmented image to obtain the vessel centerlines. The graph nodes are extracted by finding the intersection points (pixels with more than two neighbors), the endpoints (pixels with just one neighbor) and the high curvature points. Each link in the graph represents a connection between two nodes. The extracted graph may include some misrepresentations of the vascular structure as result of the segmentation and the centerline extraction processes. The typical errors are (1) splitting of one node into two nodes; (2) missing link on a side of a node; (3) incorrect detected link. In order to improve the accuracy, the extracted graph should be modified when one of these errors is identified. The final graph after applying the necessary modifications is shown in Figure 2(c).

2.2 Graph analysis

In the graph analysis phase a decision on the type of the nodes is made and based on node type, the links in the separate sub-graphs will be classified into one of two classes (C_1 and C_2). At the end of this phase we know which links are in the same class and in the next phase the artery/vein classes will be finally assigned to C_1 and C_2 . We have considered four different types of nodes: 1) Connecting points; 2) Crossing points; 3) Bifurcation points; and 4) Meeting points.

The node classification algorithm uses the following node information: the number of links connected to each node (node degree); the direction of the links; the angles between the links; the vessel caliber related to each link and the degree of adjacent nodes.

The link classification is done for each separate sub-graph and distinct classes are assigned to each region. This means that classes C_1 , C_2 will be assigned for the links in sub-graph 1, classes C_3 , C_4 for the links in sub-graph 2 and so on. For each separate sub-graph, the farthest link from OD center is detected, and a class is assigned to this link (for instance C_1); the node connected to this link is found and based on the node type the other links are labeled as class 1 or class 2. This procedure is repeated for all nodes until there is no more unclassified links. We will repeat the process for other separate sub-graphs each time defining two new classes, until the entire graph is classified. In the end we have a classified graph with different pair of classes for each disjoint sub-graph.

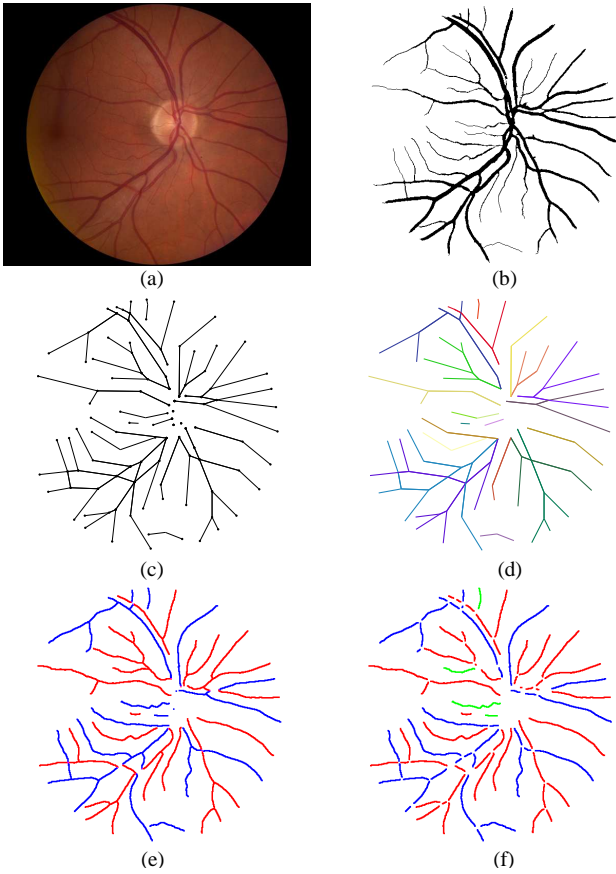


Figure 2: (a) Original color image; (b) Segmented vessels result; (c) Extracted graph; (d) Graph analysis result; (e) A/V classification result; (f) Comparison of proposed method with manual classification.

2.3 A/V classification

The purpose of this last phase is to assign the artery or the vein classes to the pair of classes in each separate sub-graph using a classifier. Having this purpose in mind, we have defined a set of features and a classifier. For each centerline pixel, the set of 30 features described in Table 1 are measured. We have used linear discriminant analysis (LDA) classifier and for feature selection, a sequential forward floating approach is used, which starts with an empty feature set and adds or removes features when this improves the performance of the classifier. After using this feature selection method a set of 19 features, 1-2, 7, 10, 12-14, 16-17, 19-20 and 23-30 was selected.

The trained classifier was used for assigning the A/V classes to the graph classes. First each centerline pixel is classified into A/V classes, then for each class (C_i) in a sub-graph, the probability of being artery is calculated based on the number of associated centerline pixels classified as an artery or a vein. The probability of a class (C_i) to be artery ($P_a(C_i)$) is computed as $P_a(C_i) = n_{C_i}^a / (n_{C_i}^a + n_{C_i}^v)$ where $n_{C_i}^a$ is the number of centerline pixels of class (C_i) classified as artery and $n_{C_i}^v$ is the number of centerline pixels classified as a vein. For each pair of classes in a separate sub-graph, the class with higher artery probability will be assigned as artery class and the other one as vein class. The result of assigning a class to the link centerline pixels is shown in Figure 2(e). The differences between the results of proposed method and manual labeling are shown in green in Figure 2(f) while the correctly classified arteries and veins are presented in red and blue respectively.

Table 1: The list of features extracted for each centerline pixel.

Nr.	Features
1-3	Normalized Red, Green and Blue intensities under the centerline pixel.
4-6	Normalized Hue, Saturation and Intensity under the centerline pixel.
7-9	Normalized mean of Red, Green and Blue intensities across the vessel.
10-12	Normalized mean of Hue, Saturation and Intensity across the vessel.
13-15	Standard deviation of Red, Green and Blue intensities across the vessel.
16-18	Standard deviation Hue, Saturation and Intensity across the vessel.
19-22	Maximum and minimum of Red and Green intensities across the vessel.
23-30	Intensity under the centerline pixel in a Gaussian blurred ($\sigma = 2, 4, 8, 16$) of Red and Green plane.

3 Evaluation and results

For validating the proposed method we have used the INSPIRE-AVR dataset which contains 40 high resolution color images with 2392×2048 pixels [13]. The manual artery/vein labeling is done by an expert for all 40 images. For evaluating the classification method, we have calculated the accuracy both for centerline pixel classification and vessel pixel classification. Table 2 shows the accuracy values for centerline pixels and for vessel pixels in the entire image and also for the pixels inside the region of interest (ROI) which is the standard ring area within 0.5 to 1.0 disc diameter from the OD margin. Each row contains the accuracy values calculated using different ranges for vessel calibers. First row is the result for all the vessels, while the remaining rows present the results for the vessels with caliber higher than 5, 10, 15 and 20 pixels.

Table 2: Accuracy rates of correctly classified pixels.

	Centerline pixels in entire image	All vessel pixels in entire image	Centerline pixels inside ROI	All vessel pixels inside ROI
All vessels	84,8%	88,0%	85,2%	90,3%
Vessels Caliber > 5 pixels	86,5%	88,4%	87,5%	90,8%
Vessels Caliber > 10 pixels	88,6%	89,4%	90,7%	92,3%
Vessels Caliber > 15 pixels	90,2%	90,4%	93,3%	94,1%
Vessels Caliber > 20 pixels	91,3%	91,1%	96,0%	96,0%

4 Conclusion

We have developed an automatic method to classify the retinal vessels into arteries and veins. We have reached an accuracy of 88.0% for correctly classified vessel pixels of entire vascular tree and an accuracy of 90.3% inside the ROI. The results show an improvement compare to previous techniques and demonstrate that the proposed automatic methodology for A/V classification is reliable for AVR calculation.

Acknowledgements

This work was financed by FEDER funds through the *Programa Operacional Factores de Competitividade – COMPETE* and by Portuguese funds through FCT – *Fundação para a Ciência e a Tecnologia* in the framework of the project PEst-C/SAU/LA0002/2011 and the research grant SFRH /BD/73376/2010.

References

- [1] T. T. Nguyen and T. Y. Wong, "Retinal vascular changes and diabetic retinopathy," *Current Diabetes Reports*, vol. 9, no. 4, pp. 277-283, 2009.
- [2] G.uan, K. Hudson, C. Wong, T. Kisilevsky, M. Nrusimhadevara, R. K. Lam, W. C. Mandelcorn, M. Devenyi, R. G. Flanagan, J. G., "Retinal hemodynamics in early diabetic macular edema," *Diabetes New York*, Vol. 55; no. 3, pp. 813, 2006.
- [3] A. S. Neubauer, M. Ludtke, C. Haritoglou, S. Priglinger and A. Kampik, "Retinal vessel analysis reproducibility in assessing cardiovascular disease," *Optometry and Vision Science*, vol. 85, no. 4, pp. E247-E254, Apr. 2008.
- [4] S. R. Lesage, T. H. Mosley, T. Y. Wong, M. Szklo, D. Knopman, D. J. Catellier, S. R. Cole, R. Klein, J. Coresh, L. H. Coker, and A. R. Sharrett, "Retinal microvascular abnormalities and cognitive decline: the ARIC 14-year follow-up study," *Neurology*, vol. 73, no. 11, pp. 862-8, 2009.
- [5] C. Sun, J. J. Wang, D. A. Mackey, and T. Y. Wong, "Retinal vascular caliber: systemic, environmental, and genetic associations," *Survey of ophthalmology*, vol. 54, pp. 74-95, 2009.
- [6] M. D. Knudtson, K. E. Lee, L. D. Hubbard, T. Y. Wong, R. Klein, and B. E. Klein, "Revised formulas for summarizing retinal vessel diameters," *Current eye research*, vol. 27, pp. 143-9, 2003.
- [7] K. Rothaus, P. Rhiem, and X. Jiang, "Separation of the Retinal Vascular Graph in Arteries and Veins," in *LNCS*, 4538, pp. 251-262, 2007.
- [8] E. Grisan and A. Ruggeri, "A divide et impera strategy for automatic classification of retinal vessels into arteries and veins," *Proc. 25th Annual IEEE Int. Conf. Engineering in Medicine and Biology Society*, pp. 890-893, 2003.
- [9] M. Niemeijer, B. van Ginneken, and M. D. Abramoff, "Automatic classification of retinal vessels into arteries and veins," *Proceedings of SPIE*, vol. 7260, p. 72601F-72601F-8, 2009.
- [10] S. G. Vázquez, N. Barreira, M. G. Penedo, M. Ortega, and a. Pose-Reino, "Improvements in retinal vessel clustering techniques: towards the automatic computation of the arterio venous ratio," *Computing*, vol. 90, no. 3-4, pp. 197-217, Aug. 2010.
- [11] Richard S. Snell and Michael A. Lemp, "Clinical anatomy of the eye," Wiley-Blackwell, January 1998.
- [12] A.M. Mendonça and A. Campilho, "Segmentation of retinal blood vessels by combining the detection of centerlines and morphological reconstruction," *IEEE Trans. Med. Imag.*, vol. 25, pp. 1200-13, Sep. 2006.
- [13] <http://webye.ophth.uiowa.edu/component/k2/item/270>.